



Received 15 November 2018
Accepted 16 November 2018

Edited by D.-J. Xu, Zhejiang University (Yuquan Campus), China

Keywords: crystal structure; benzodiazole; hydrogen bond; alkyne; Hirshfeld surface.

CCDC reference: 1879758

Supporting information: this article has supporting information at journals.iucr.org/e

Crystal structure and Hirshfeld surface analysis of 1-benzyl-3-(prop-2-yn-1-yl)-2,3-dihydro-1*H*-1,3-benzodiazol-2-one

Asmaa Saber,^{a*} Nada Kheira Sebbar,^b Tuncer Hökelek,^c Mohamed El hafi,^a Joel T. Mague^d and El Mokhtar Essassi^a

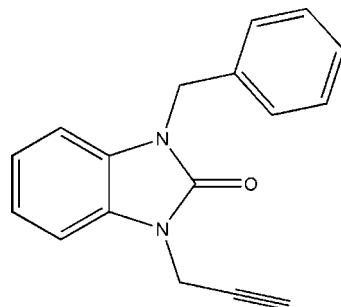
^aLaboratoire de Chimie Organique Hétérocyclique URAC 21, Pôle de Compétence Pharmacochimie, Av. Ibn Battouta, BP 1014, Faculté des Sciences, Université Mohammed V, Rabat, Morocco, ^bLaboratoire de Chimie Bioorganique Appliquée, Faculté des Sciences, Université Ibn Zohr, Agadir, Morocco, ^cDepartment of Physics, Hacettepe University, 06800 Beytepe, Ankara, Turkey, and ^dDepartment of Chemistry, Tulane University, New Orleans, LA 70118, USA.

*Correspondence e-mail: as.saber.pro@gmail.com

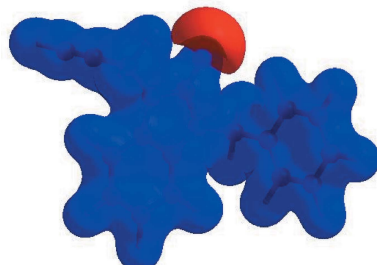
The title compound, $C_{17}H_{14}N_2O$, is built up from the planar benzodiazole unit linked to the benzyl and propynyl substituents. The substituents are rotated significantly out of the benzodiazole plane, where the benzyl group is inclined by $68.91(7)^\circ$ to the benzodiazole unit. In the crystal, the molecules are linked via intermolecular $C-H_{Bnzdzl}\cdots O$ and $C-H_{Bnzy}\cdots O$ ($Bnzdzl$ = benzodiazole and $Bnzy$ = benzyl) hydrogen bonds, enclosing $R_4^4(27)$ ring motifs, into a network consisting of rectangular layers parallel to the bc plane which are also stacked along the a -axis direction being associated through $C-H\cdots \pi$ (ring) interactions. The Hirshfeld surface analysis of the crystal structure indicates that the most important contributions for the crystal packing are from $H\cdots H$ (43.6%), $H\cdots C/C\cdots H$ (42.0%) and $H\cdots O/O\cdots H$ (8.9%) interactions.

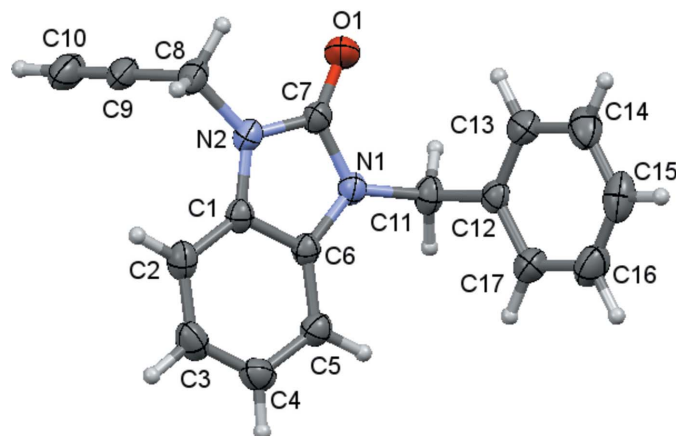
1. Chemical context

The benzimidazole nucleus constitutes an important pharmacophore in medicinal chemistry and pharmacology (Ouzidan *et al.*, 2011; Dardouri *et al.*, 2011; Soderlind *et al.*, 1999). Benzimidazol-2-one derivatives are of wide interest because of their diverse biological activities such as anti-microbial, anti-fungal, anti-histaminic, anti-inflammatory, antiviral and anti-oxidant (Walia *et al.*, 2011; Luo *et al.*, 2011; Ayhan-Kılçığlı *et al.*, 2007; Navarrete-Vázquez *et al.*, 2001).



As a continuation of our research works devoted to the development of substituted benzimidazol-2-one derivatives (Lakhrissi *et al.*, 2008; Mondieig *et al.*, 2013), we report herein the synthesis, the molecular and crystal structures along with the Hirshfeld surface analysis of a new benzimidazol-2-one derivative, namely 2-benzyl-1-(prop-2-ynyl)-1*H*-benzoimidazol 2(*H*)-one. It was obtained by condensation of benzyl chloride with 1-(prop-2-ynyl)-1*H*-benzoimidazol-2(*H*)-one in



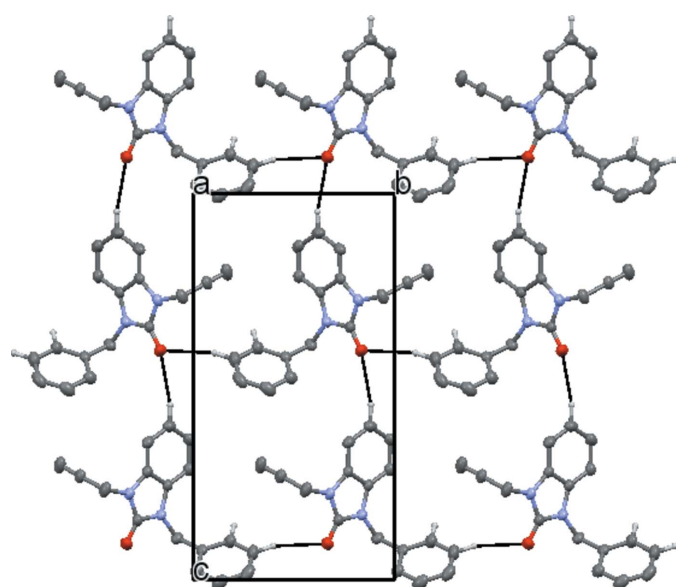
**Figure 1**

The molecular structure of the title compound with the atom-numbering scheme. Displacement ellipsoids are drawn at the 30% probability level.

the presence of tetra-*n*-butylammonium bromide as catalyst and potassium carbonate as base.

2. Structural commentary

The title compound is built up from a benzodiazole unit linked to benzyl and propynyl substituents (Fig. 1). The benzodiazole moiety is planar to within 0.015 (1) Å (for atom C7), and the r.m.s. deviation of the fitted atoms is 0.008 Å. It is inclined by 68.91 (7)° to the C12–C17 ring plane. The benzyl substituent is nearly perpendicular to the benzodiazole plane, as indicated by the C6–N1–C11–C12 torsion angle of –87.00 (15)° while the propynyl substituent is at a smaller angle [C1–N2–C8–C9 = –73.46 (18)°]. Atoms O1, C8 and C11 deviate by 0.038 (1), 0.003 (2) and 0.047 (2) Å, respectively, from the benzodiazole plane.

**Figure 2**

Plan view of a portion of one layer seen along the *a*-axis direction. Intermolecular C–H_{Bnzdzl}···O and C–H_{Bnzy}···O (Bnzdzl = benzodiazole and Bnzy = benzyl) hydrogen bonds are shown by dashed lines.

Table 1
Hydrogen-bond geometry (Å, °).

Cg2 is the centroid of the C1–C6 benzene ring.

D–H···A	D–H	H···A	D···A	D–H···A
C3–H3···O1 ⁱⁱⁱ	0.982 (18)	2.542 (18)	3.4997 (18)	165.1 (14)
C16–H16···O1 ^{vi}	0.994 (18)	2.568 (18)	3.468 (2)	150.6 (14)
C17–H17···Cg2 ^{viii}	1.00 (2)	2.831 (18)	3.6964 (17)	144.6 (15)

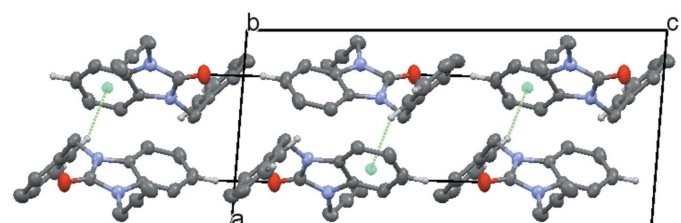
Symmetry codes: (iii) $x, -y + \frac{3}{2}, z - \frac{1}{2}$; (vi) $x, y - 1, z$; (viii) $-x + 1, y - \frac{1}{2}, -z + \frac{1}{2}$.

3. Supramolecular features

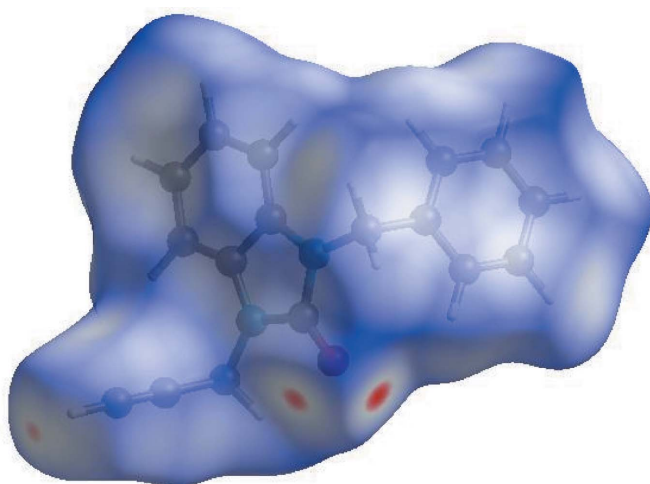
In the crystal, the molecules are linked via intermolecular C–H_{Bnzdzl}···O and C–H_{Bnzy}···O (Bnzdzl = benzodiazole and Bnzy = benzyl) hydrogen bonds (Table 1), enclosing $R_4^4(27)$ ring motifs, into a network consisting of rectangular layers parallel to the *bc* plane (Fig. 2), which stack along the *a*-axis direction being associated through C–H···π (ring) interactions (Fig. 3).

4. Hirshfeld surface analysis

In order to visualize the intermolecular interactions in the crystal of the title compound, a Hirshfeld surface (HS) analysis (Hirshfeld, 1977; Spackman & Jayatilaka, 2009) was carried out using *CrystalExplorer17.5* (Turner *et al.*, 2017). In the HS plotted over d_{norm} (Fig. 4), the white surface indicates contacts with distances equal to the sum of van der Waals radii, and the red and blue colours indicate distances shorter (in close contact) or longer (distinct contact) than the van der Waals radii, respectively (Venkatesan *et al.*, 2016). The bright-red spot appearing near O1 indicates its role as acceptor in the dominant C–H···O hydrogen bonds. Hydrogen-bond donors and acceptors appear, respectively, as blue and red regions corresponding to positive and negative potentials on the HS mapped over electrostatic potential (Spackman *et al.*, 2008; Jayatilaka *et al.*, 2005) shown in Fig. 5. The shape-index of the HS is a tool to visualize the π–π stacking by the presence of adjacent red and blue triangles; if there are no adjacent red and/or blue triangles, then there are no π–π interactions. Fig. 6 clearly suggests that there are no π–π interactions present. The overall two-dimensional fingerprint plot, Fig. 7(a), and those delineated into H···H, H···C/C···H, H···O/O···H, H···N/N···H, C···C and N···C/C···N contacts (McKinnon *et*

**Figure 3**

Elevation view of two layers seen along the *b*-axis direction. C–H···O hydrogen bonds are shown by black dashed lines while C–H···π(ring) interactions are shown by green dashed lines.

**Figure 4**

View of the three-dimensional Hirshfeld surface of the title compound plotted over d_{norm} in the range -0.1150 to 1.2702 a.u.

al., 2007) are illustrated in Fig. 7(b)–(g), respectively, together with their relative contributions to the Hirshfeld surface. The most important interaction type is H···H, contributing 43.6% to the overall crystal packing, which is reflected in Fig. 7(b) as widely scattered points of high density due to the large hydrogen content of the molecule and also due to the short H···H contacts (Table 2). In the presence of C—H··· π interactions, the pair of widely scattered points of wings in the fingerprint plot delineated into H···C/C···H contacts (42.0% contribution to the HS) have a nearly symmetrical distribution of points, Fig. 7(c), with the tips at $d_e + d_i \sim 2.72$ Å. The pair of characteristic wings in the fingerprint plot delineated into H···O/O···H contacts (8.9% contribution), Fig. 7(d), arises from the C—H···O hydrogen bonds (Table 1) as well as from

Table 2
Selected interatomic distances (Å).

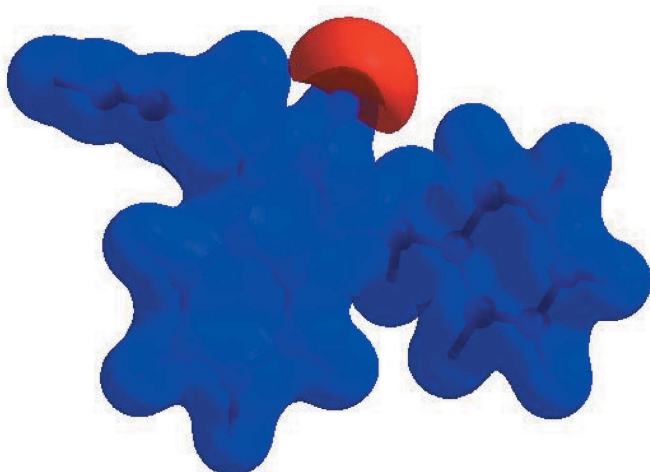
O1···H8 <i>B</i>	2.492 (18)	C5···H11 <i>A</i>	2.897 (16)
O1···H11 <i>B</i>	2.607 (16)	C5···H10 ^{vi}	2.93 (3)
O1···H13	2.760 (18)	C8···H2	2.947 (16)
O1···H16 ⁱ	2.568 (18)	C10···H8 <i>A</i> ⁱⁱ	2.874 (18)
C2···C9	3.5265 (19)	C10···H14 ⁱⁱⁱ	2.95 (2)
C7···C13	3.5805 (19)	C10···H11 <i>A</i> ^{vii}	2.895 (17)
C9···C1 ⁱⁱ	3.5236 (18)	C11···H5	2.998 (16)
C10···N2 ⁱⁱ	3.4291 (19)	C13···H14 ^v	2.964 (17)
C10···C8 ⁱⁱ	3.385 (2)	H3···O1 ⁱⁱⁱ	2.542 (18)
C10···C14 ⁱⁱⁱ	3.512 (3)	H5···H11 <i>A</i>	2.46 (2)
C11···C13 ^{iv}	3.495 (2)	H11 <i>A</i> ···H17	2.38 (2)
C14···C14 ^v	3.543 (2)	H11 <i>B</i> ···H13	2.45 (2)
C4···H10 ^{vi}	2.84 (3)		

Symmetry codes: (i) $x, y+1, z$; (ii) $-x, y+\frac{1}{2}, -z+\frac{1}{2}$; (iii) $x, -y+\frac{3}{2}, z-\frac{1}{2}$; (iv) $-x+1, -y+1, -z+1$; (v) $-x, -y+1, -z+1$; (vi) $x, y-1, z$; (vii) $-x+1, y+\frac{1}{2}, -z+\frac{1}{2}$.

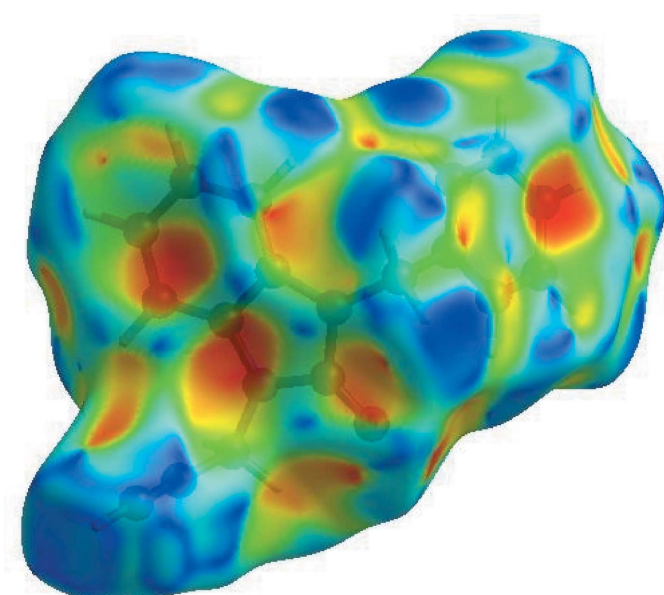
the H···O/O···H contacts (Table 3) and has a pair of spikes with the tips at $d_e + d_i = 2.43$ Å. The pair of characteristic wings resulting in the fingerprint plot delineated into H···N/N···H contacts [Fig. 7(e), 2.5% contribution] has a pair of spikes with the tips at $d_e + d_i = 3.12$ Å. Finally, the wide spike with the tip at $d_e = d_i = 1.77$ Å in Fig. 7(f) is due to the C···C contacts (Table 3).

The Hirshfeld surface representations with the function d_{norm} plotted onto the surface are shown for the H···H, H···C/C···H, H···O/O···H and H···O/O···H interactions in Fig. 8(a)–(d), respectively.

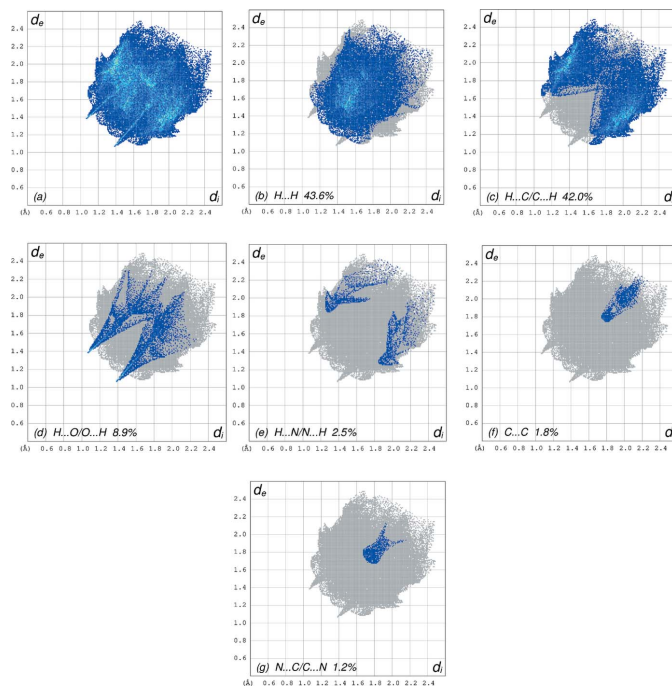
The Hirshfeld surface analysis confirms the importance of H-atom contacts in establishing the packing. The large number of H···H, H···O/O···H and H···C/C···H interactions suggest that van der Waals interactions and hydrogen bonding play the major roles in the crystal packing (Hathwar *et al.*, 2015).

**Figure 5**

View of the three-dimensional Hirshfeld surface of the title compound plotted over electrostatic potential energy in the range -0.0500 to 0.0500 a.u. using the STO-3 G basis set at the Hartree–Fock level of theory. Hydrogen-bond donors and acceptors are shown as blue and red regions around the atoms corresponding to positive and negative potentials, respectively.

**Figure 6**

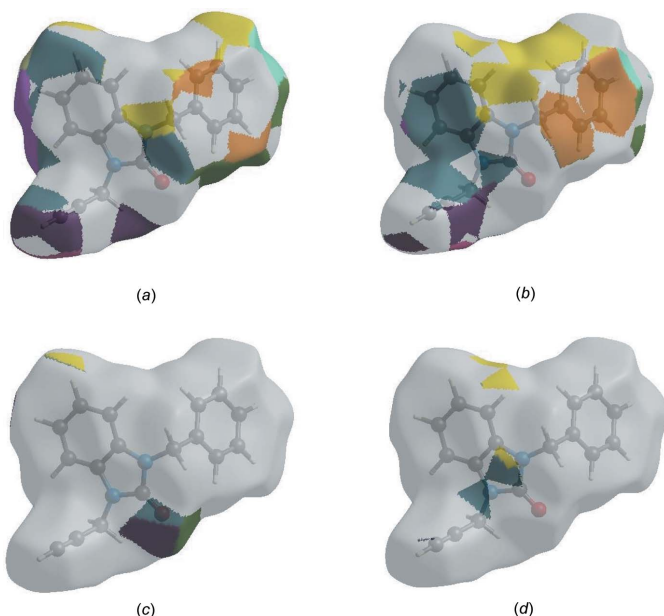
Hirshfeld surface of the title compound plotted over shape-index.

**Figure 7**

The full two-dimensional fingerprint plots for the title compound, showing (a) all interactions, and those delineated into (b) H···H, (c) H···C/C···H, (d) H···O/O···H, (e) H···N/N···H, (f) C···C and (g) N···C/C···N interactions. The d_i and d_e values are the closest internal and external distances (in Å) from given points on the Hirshfeld surface contacts.

5. Synthesis and crystallization

To a solution of 1-(prop-2-ynyl)-1*H*-benzimidazol-2(3*H*)-one (3.42 mmol), benzyl chloride (6.81 mmol) and potassium

**Figure 8**

The Hirshfeld surface representations with the function d_{norm} plotted onto the surface for (a) H···H, (b) H···C/C···H, (c) H···O/O···H and (d) H···N/N···H interactions.

Table 3
Experimental details.

Crystal data	$C_{17}H_{14}N_2O$
Chemical formula	
M_r	262.30
Crystal system, space group	Monoclinic, $P2_1/c$
Temperature (K)	298
a, b, c (Å)	8.3567 (2), 9.2040 (2), 17.7868 (4)
β (°)	94.559 (1)
V (Å ³)	1363.74 (5)
Z	4
Radiation type	Cu $K\alpha$
μ (mm ⁻¹)	0.64
Crystal size (mm)	0.23 × 0.20 × 0.19
Data collection	Bruker D8 VENTURE PHOTON 100 CMOS
Diffractometer	Multi-scan (<i>SADABS</i> ; Krause <i>et al.</i> , 2015)
Absorption correction	0.86, 0.89
T_{min}, T_{max}	13551, 2778, 2433
No. of measured, independent and observed [$I > 2\sigma(I)$] reflections	0.032
R_{int}	0.625
(sin θ/λ) _{max} (Å ⁻¹)	
Refinement	
$R[F^2 > 2\sigma(F^2)], wR(F^2), S$	0.038, 0.108, 1.05
No. of reflections	2778
No. of parameters	238
H-atom treatment	All H-atom parameters refined
$\Delta\rho_{max}, \Delta\rho_{min}$ (e Å ⁻³)	0.15, -0.12

Computer programs: *APEX3* and *SAINT* (Bruker, 2016), *SHELXT* (Sheldrick, 2015a), *SHELXL2018/1* (Sheldrick, 2015b), *Mercury* (Macrae, *et al.*, 2008) and *SHELXTL* (Sheldrick, 2008).

carbonate (6.42 mmol) in DMF (15 ml) was added a catalytic amount of tetra-*n*-butylammonium bromide (0.37 mmol) and the mixture was stirred for 24 h. The solid material was removed by filtration and the solvent evaporated under vacuum. The solid product was purified by recrystallization from ethanol to afford colourless crystals in 76% yield.

6. Refinement

Crystal data, data collection and structure refinement details are summarized in Table 3. Hydrogen atoms were located in a difference-Fourier map and freely refined.

Funding information

The support of NSF–MRI grant No. 1228232 for the purchase of the diffractometer and Tulane University for support of the Tulane Crystallography Laboratory are gratefully acknowledged. TH is grateful to Hacettepe University Scientific Research Project Unit (grant No. 013 D04 602 004).

References

- Ayhan-Kılçgil, G., Kus, G., Özdamar, E. D., Can-Eke, B. & Iscan, M. (2007). *Arch. Pharm. Chem. Life Sci.* **340**, 607–611.
- Bruker (2016). *APEX3* and *SAINT*. Bruker AXS Inc., Madison, Wisconsin, USA.
- Dardouri, R., Rodi, Y. K., Saffon, N., Essassi, E. M. & Ng, S. W. (2011). *Acta Cryst. E67*, o1853.

- Hathwar, V. R., Sist, M., Jørgensen, M. R. V., Mamakhet, A. H., Wang, X., Hoffmann, C. M., Sugimoto, K., Overgaard, J. & Iversen, B. B. (2015). *IUCrJ*, **2**, 563–574.
- Hirshfeld, H. L. (1977). *Theor. Chim. Acta*, **44**, 129–138.
- Jayatilaka, D., Grimwood, D. J., Lee, A., Lemay, A., Russel, A. J., Taylor, C., Wolff, S. K., Cassam-Chenai, P. & Whitton, A. (2005). TONTO - A System for Computational Chemistry. Available at: <http://hirshfeldsurface.net/>
- Krause, L., Herbst-Irmer, R., Sheldrick, G. M. & Stalke, D. (2015). *J. Appl. Cryst.* **48**, 3–10.
- Lakhrissi, B., Benksim, A., Massouli, M., Essassi, el M., Lequart, V., Joly, N., Beaupère, D., Wadouachi, A. & Martin, P. (2008). *Carbohydr. Res.* **343**, 421–433.
- Luo, Y., Yao, J.-P., Yang, L., Feng, C.-L., Tang, W., Wang, G.-F., Zuo, J.-P. & Lu, W. (2011). *Arch. Pharm. Pharm. Med. Chem.* **344**, 78–83.
- Macrae, C. F., Bruno, I. J., Chisholm, J. A., Edgington, P. R., McCabe, P., Pidcock, E., Rodriguez-Monge, L., Taylor, R., van de Streek, J. & Wood, P. A. (2008). *J. Appl. Cryst.* **41**, 466–470.
- McKinnon, J. J., Jayatilaka, D. & Spackman, M. A. (2007). *Chem. Commun.* pp. 3814–3816.
- Mondieig, D., Lakhrissi, L., El Assyry, A., Lakhrissi, B., Negrier, P., Essassi, E. M., Massouli, M., Michel Leger, J. & Benali, B. (2013). *J. Mar. Chim. Heterocycl.* **12**, 51–61.
- Navarrete-Vázquez, G., Cedillo, R., Hernández-Campos, A., Yépez, L., Hernández-Luis, F., Valdez, J., Morales, R., Cortés, R., Hernández, M. & Castillo, R. (2001). *Bioorg. Med. Chem.* **11**, 187–190.
- Ouzidan, Y., Kandri Rodi, Y., Fronczek, F. R., Venkatraman, R., El Ammari, L. & Essassi, E. M. (2011). *Acta Cryst. E* **67**, o362–o363.
- Sheldrick, G. M. (2008). *Acta Cryst. A* **64**, 112–122.
- Sheldrick, G. M. (2015a). *Acta Cryst. A* **71**, 3–8.
- Sheldrick, G. M. (2015b). *Acta Cryst. C* **71**, 3–8.
- Soderlind, K. J., Gorodetsky, B., Singh, A. K., Bachur, N., Miller, G. G. & Lown, J. W. (1999). *Anticancer Drug Des.* **14**, 19–36.
- Spackman, M. A. & Jayatilaka, D. (2009). *CrystEngComm*, **11**, 19–32.
- Spackman, M. A., McKinnon, J. J. & Jayatilaka, D. (2008). *CrystEngComm*, **10**, 377–388.
- Turner, M. J., McKinnon, J. J., Wolff, S. K., Grimwood, D. J., Spackman, P. R., Jayatilaka, D. & Spackman, M. A. (2017). *CrystalExplorer17*. The University of Western Australia.
- Venkatesan, P., Thamotharan, S., Ilangoan, A., Liang, H. & Sundius, T. (2016). *Spectrochim. Acta Part A*, **153**, 625–636.
- Walia, R., Hedaitullah, M., Naaz, S. F., Iqbal, K. & Lamba, H. S. (2011). *Int. J. Res. Pharm. & Chem.* **1**, 565–574.

supporting information

Acta Cryst. (2018). E74, 1842-1846 [https://doi.org/10.1107/S2056989018016298]

Crystal structure and Hirshfeld surface analysis of 1-benzyl-3-(prop-2-yn-1-yl)-2,3-dihydro-1*H*-1,3-benzodiazol-2-one

Asmaa Saber, Nada Kheira Sebbar, Tuncer Hökelek, Mohamed El hafi, Joel T. Mague and El Mokhtar Essassi

Computing details

Data collection: *APEX3* (Bruker, 2016); cell refinement: *SAINT* (Bruker, 2016); data reduction: *SAINT* (Bruker, 2016); program(s) used to solve structure: *SHELXT* (Sheldrick, 2015a); program(s) used to refine structure: *SHELXL2018/1* (Sheldrick, 2015b); molecular graphics: *Mercury* (Macrae, *et al.*, 2008); software used to prepare material for publication: *SHELXTL* (Sheldrick, 2008).

1-Benzyl-3-(prop-2-yn-1-yl)-2,3-dihydro-1*H*-1,3-benzodiazol-2-one

Crystal data

C₁₇H₁₄N₂O
 $M_r = 262.30$
 Monoclinic, $P2_1/c$
 $a = 8.3567 (2)$ Å
 $b = 9.2040 (2)$ Å
 $c = 17.7868 (4)$ Å
 $\beta = 94.559 (1)^\circ$
 $V = 1363.74 (5)$ Å³
 $Z = 4$

$F(000) = 552$
 $D_x = 1.278 \text{ Mg m}^{-3}$
 Cu $K\alpha$ radiation, $\lambda = 1.54178$ Å
 Cell parameters from 9908 reflections
 $\theta = 2.5\text{--}74.9^\circ$
 $\mu = 0.64 \text{ mm}^{-1}$
 $T = 298 \text{ K}$
 Block, colourless
 $0.23 \times 0.20 \times 0.19$ mm

Data collection

Bruker D8 VENTURE PHOTON 100 CMOS
 diffractometer
 Radiation source: INCOATEC I μ S micro-focus
 source
 ω scans
 Absorption correction: multi-scan
 (*SADABS*; Krause *et al.*, 2015)
 $T_{\min} = 0.86$, $T_{\max} = 0.89$

13551 measured reflections
 2778 independent reflections
 2433 reflections with $I > 2\sigma(I)$
 $R_{\text{int}} = 0.032$
 $\theta_{\max} = 74.4^\circ$, $\theta_{\min} = 5.0^\circ$
 $h = -10 \rightarrow 10$
 $k = -11 \rightarrow 11$
 $l = -22 \rightarrow 21$

Refinement

Refinement on F^2
 Least-squares matrix: full
 $R[F^2 > 2\sigma(F^2)] = 0.038$
 $wR(F^2) = 0.108$
 $S = 1.05$
 2778 reflections
 238 parameters
 0 restraints

Primary atom site location: structure-invariant
 direct methods
 Secondary atom site location: difference Fourier
 map
 Hydrogen site location: difference Fourier map
 All H-atom parameters refined
 $w = 1/[\sigma^2(F_o^2) + (0.0559P)^2 + 0.1595P]$
 where $P = (F_o^2 + 2F_c^2)/3$
 $(\Delta/\sigma)_{\max} < 0.001$

$\Delta\rho_{\max} = 0.15 \text{ e Å}^{-3}$
 $\Delta\rho_{\min} = -0.12 \text{ e Å}^{-3}$

Extinction correction: *SHELXL-2018/1*
(Sheldrick, 2015*b*),
 $F_c^* = k F_c [1 + 0.001 x F_c^2 \lambda^3 / \sin(2\theta)]^{-1/4}$
Extinction coefficient: 0.0123 (10)

Special details

Geometry. All esds (except the esd in the dihedral angle between two l.s. planes) are estimated using the full covariance matrix. The cell esds are taken into account individually in the estimation of esds in distances, angles and torsion angles; correlations between esds in cell parameters are only used when they are defined by crystal symmetry. An approximate (isotropic) treatment of cell esds is used for estimating esds involving l.s. planes.

Refinement. Refinement of F^2 against ALL reflections. The weighted R-factor wR and goodness of fit S are based on F^2 , conventional R-factors R are based on F , with F set to zero for negative F^2 . The threshold expression of $F^2 > 2\sigma(F^2)$ is used only for calculating R-factors(gt) etc. and is not relevant to the choice of reflections for refinement. R-factors based on F^2 are statistically about twice as large as those based on F , and R-factors based on ALL data will be even larger.

Fractional atomic coordinates and isotropic or equivalent isotropic displacement parameters (\AA^2)

	x	y	z	$U_{\text{iso}}^*/U_{\text{eq}}$
O1	0.22681 (15)	0.83445 (11)	0.40629 (6)	0.0792 (3)
N1	0.34376 (12)	0.66295 (10)	0.33147 (5)	0.0533 (3)
N2	0.17477 (12)	0.82074 (10)	0.27629 (6)	0.0543 (3)
C1	0.22401 (13)	0.73060 (12)	0.22001 (6)	0.0491 (3)
C2	0.18494 (17)	0.72757 (15)	0.14354 (7)	0.0629 (3)
H2	0.1121 (19)	0.7990 (18)	0.1214 (9)	0.075 (4)*
C3	0.2547 (2)	0.62075 (18)	0.10228 (8)	0.0734 (4)
H3	0.234 (2)	0.617 (2)	0.0472 (10)	0.090 (5)*
C4	0.3609 (2)	0.52123 (16)	0.13680 (8)	0.0703 (4)
H4	0.414 (2)	0.4500 (18)	0.1060 (9)	0.077 (4)*
C5	0.40140 (16)	0.52408 (14)	0.21399 (8)	0.0590 (3)
H5	0.476 (2)	0.4532 (18)	0.2392 (9)	0.077 (4)*
C6	0.33092 (13)	0.63007 (12)	0.25513 (6)	0.0478 (3)
C7	0.24590 (16)	0.77932 (13)	0.34550 (7)	0.0555 (3)
C8	0.06278 (18)	0.94116 (15)	0.26623 (10)	0.0675 (4)
H8A	-0.034 (2)	0.908 (2)	0.2331 (11)	0.095 (6)*
H8B	0.030 (2)	0.965 (2)	0.3179 (11)	0.089 (5)*
C9	0.13423 (17)	1.06640 (14)	0.23111 (8)	0.0633 (3)
C10	0.1922 (2)	1.16568 (17)	0.20289 (11)	0.0854 (5)
H10	0.236 (3)	1.249 (3)	0.1798 (13)	0.132 (8)*
C11	0.43747 (17)	0.58361 (15)	0.39115 (8)	0.0600 (3)
H11A	0.539 (2)	0.5429 (18)	0.3684 (9)	0.080 (5)*
H11B	0.4649 (19)	0.6538 (18)	0.4327 (10)	0.080 (5)*
C12	0.34639 (14)	0.45907 (12)	0.42256 (6)	0.0512 (3)
C13	0.23968 (18)	0.48403 (17)	0.47628 (8)	0.0675 (4)
H13	0.223 (2)	0.587 (2)	0.4938 (9)	0.087 (5)*
C14	0.1570 (2)	0.3702 (2)	0.50568 (10)	0.0819 (5)
H14	0.086 (2)	0.387 (2)	0.5429 (12)	0.107 (6)*
C15	0.1808 (2)	0.2308 (2)	0.48218 (11)	0.0830 (5)
H15	0.123 (2)	0.154 (2)	0.5025 (10)	0.095 (6)*
C16	0.2874 (3)	0.20500 (18)	0.42939 (11)	0.0870 (5)

H16	0.306 (2)	0.104 (2)	0.4124 (11)	0.106 (6)*
C17	0.3696 (2)	0.31841 (15)	0.39958 (9)	0.0701 (4)
H17	0.446 (2)	0.299 (2)	0.3599 (12)	0.103 (6)*

Atomic displacement parameters (\AA^2)

	U^{11}	U^{22}	U^{33}	U^{12}	U^{13}	U^{23}
O1	0.1247 (9)	0.0571 (6)	0.0569 (5)	0.0079 (5)	0.0134 (5)	-0.0057 (4)
N1	0.0663 (6)	0.0445 (5)	0.0475 (5)	0.0034 (4)	-0.0042 (4)	0.0037 (4)
N2	0.0612 (6)	0.0435 (5)	0.0583 (6)	0.0059 (4)	0.0049 (4)	0.0066 (4)
C1	0.0519 (6)	0.0436 (6)	0.0512 (6)	-0.0061 (4)	0.0006 (4)	0.0055 (4)
C2	0.0717 (8)	0.0593 (7)	0.0557 (7)	-0.0085 (6)	-0.0081 (6)	0.0106 (6)
C3	0.1009 (11)	0.0707 (9)	0.0478 (7)	-0.0184 (8)	0.0008 (7)	0.0001 (6)
C4	0.0940 (10)	0.0571 (8)	0.0619 (8)	-0.0090 (7)	0.0197 (7)	-0.0083 (6)
C5	0.0661 (7)	0.0469 (6)	0.0645 (7)	0.0002 (5)	0.0090 (6)	0.0013 (5)
C6	0.0524 (6)	0.0413 (5)	0.0493 (6)	-0.0050 (4)	0.0014 (4)	0.0035 (4)
C7	0.0727 (8)	0.0420 (6)	0.0520 (6)	-0.0020 (5)	0.0054 (5)	0.0027 (5)
C8	0.0649 (8)	0.0524 (7)	0.0868 (10)	0.0123 (6)	0.0158 (7)	0.0174 (7)
C9	0.0715 (8)	0.0472 (6)	0.0723 (8)	0.0125 (6)	0.0130 (6)	0.0067 (6)
C10	0.1019 (12)	0.0519 (8)	0.1070 (13)	0.0087 (8)	0.0373 (10)	0.0107 (8)
C11	0.0641 (7)	0.0574 (7)	0.0560 (7)	-0.0024 (6)	-0.0113 (6)	0.0091 (6)
C12	0.0549 (6)	0.0490 (6)	0.0478 (6)	0.0059 (5)	-0.0082 (5)	0.0057 (5)
C13	0.0748 (8)	0.0627 (8)	0.0652 (8)	0.0149 (7)	0.0066 (6)	0.0057 (6)
C14	0.0666 (8)	0.0971 (12)	0.0833 (10)	0.0159 (8)	0.0131 (8)	0.0295 (9)
C15	0.0703 (9)	0.0791 (11)	0.0967 (12)	-0.0107 (8)	-0.0120 (8)	0.0368 (9)
C16	0.1131 (14)	0.0506 (8)	0.0956 (12)	-0.0019 (8)	-0.0018 (10)	0.0065 (8)
C17	0.0896 (10)	0.0526 (7)	0.0687 (8)	0.0097 (7)	0.0099 (7)	0.0036 (6)

Geometric parameters (\AA , ^\circ)

O1—C7	1.2163 (15)	C8—H8A	1.01 (2)
N1—C7	1.3823 (16)	C8—H8B	1.004 (18)
N1—C6	1.3869 (15)	C9—C10	1.166 (2)
N1—C11	1.4632 (15)	C10—H10	0.95 (2)
N2—C7	1.3775 (16)	C11—C12	1.5076 (17)
N2—C1	1.3875 (15)	C11—H11A	1.042 (17)
N2—C8	1.4525 (16)	C11—H11B	0.995 (18)
C1—C2	1.3737 (17)	C12—C17	1.3761 (18)
C1—C6	1.3985 (16)	C12—C13	1.3771 (19)
C2—C3	1.383 (2)	C13—C14	1.381 (2)
C2—H2	0.959 (17)	C13—H13	1.008 (19)
C3—C4	1.384 (2)	C14—C15	1.369 (3)
C3—H3	0.982 (18)	C14—H14	0.94 (2)
C4—C5	1.388 (2)	C15—C16	1.366 (3)
C4—H4	0.983 (17)	C15—H15	0.94 (2)
C5—C6	1.3793 (17)	C16—C17	1.379 (2)
C5—H5	0.986 (17)	C16—H16	0.99 (2)
C8—C9	1.4610 (19)	C17—H17	1.00 (2)

O1···H8B	2.492 (18)	C5···H11A	2.897 (16)
O1···H11B	2.607 (16)	C5···H10 ^{vi}	2.93 (3)
O1···H13	2.760 (18)	C8···H2	2.947 (16)
O1···H16 ⁱ	2.568 (18)	C10···H8A ⁱⁱ	2.874 (18)
C2···C9	3.5265 (19)	C10···H14 ⁱⁱⁱ	2.95 (2)
C7···C13	3.5805 (19)	C10···H11A ^{vii}	2.895 (17)
C9···C1 ⁱⁱ	3.5236 (18)	C11···H5	2.998 (16)
C10···N2 ⁱⁱ	3.4291 (19)	C13···H14 ^v	2.964 (17)
C10···C8 ⁱⁱ	3.385 (2)	H3···O1 ⁱⁱⁱ	2.542 (18)
C10···C14 ⁱⁱⁱ	3.512 (3)	H5···H11A	2.46 (2)
C11···C13 ^{iv}	3.495 (2)	H11A···H17	2.38 (2)
C14···C14 ^v	3.543 (2)	H11B···H13	2.45 (2)
C4···H10 ^{vi}	2.84 (3)		
C7—N1—C6	110.18 (9)	N2—C8—H8B	105.8 (10)
C7—N1—C11	123.09 (10)	C9—C8—H8B	111.9 (11)
C6—N1—C11	126.62 (10)	H8A—C8—H8B	109.7 (15)
C7—N2—C1	110.34 (9)	C10—C9—C8	179.48 (16)
C7—N2—C8	123.32 (11)	C9—C10—H10	178.1 (14)
C1—N2—C8	126.34 (11)	N1—C11—C12	113.05 (10)
C2—C1—N2	131.74 (11)	N1—C11—H11A	107.8 (9)
C2—C1—C6	121.46 (11)	C12—C11—H11A	108.8 (9)
N2—C1—C6	106.80 (10)	N1—C11—H11B	107.1 (10)
C1—C2—C3	117.56 (13)	C12—C11—H11B	108.2 (9)
C1—C2—H2	119.0 (10)	H11A—C11—H11B	112.0 (13)
C3—C2—H2	123.4 (10)	C17—C12—C13	118.52 (13)
C2—C3—C4	121.16 (13)	C17—C12—C11	121.19 (12)
C2—C3—H3	120.6 (11)	C13—C12—C11	120.28 (12)
C4—C3—H3	118.2 (11)	C12—C13—C14	120.50 (15)
C3—C4—C5	121.56 (14)	C12—C13—H13	119.1 (10)
C3—C4—H4	119.7 (10)	C14—C13—H13	120.4 (10)
C5—C4—H4	118.6 (10)	C15—C14—C13	120.41 (16)
C6—C5—C4	117.22 (13)	C15—C14—H14	119.1 (14)
C6—C5—H5	120.5 (10)	C13—C14—H14	120.5 (14)
C4—C5—H5	122.3 (10)	C16—C15—C14	119.46 (16)
C5—C6—N1	132.12 (11)	C16—C15—H15	120.9 (11)
C5—C6—C1	121.03 (11)	C14—C15—H15	119.6 (11)
N1—C6—C1	106.85 (10)	C15—C16—C17	120.33 (16)
O1—C7—N2	126.95 (12)	C15—C16—H16	119.8 (12)
O1—C7—N1	127.23 (12)	C17—C16—H16	119.8 (12)
N2—C7—N1	105.82 (10)	C12—C17—C16	120.78 (15)
N2—C8—C9	111.93 (11)	C12—C17—H17	119.1 (11)
N2—C8—H8A	108.6 (11)	C16—C17—H17	120.1 (11)
C9—C8—H8A	108.8 (11)		
C7—N2—C1—C2	179.03 (13)	C1—N2—C7—N1	1.23 (13)
C8—N2—C1—C2	-0.1 (2)	C8—N2—C7—N1	-179.61 (11)

C7—N2—C1—C6	−0.58 (13)	C6—N1—C7—O1	178.85 (13)
C8—N2—C1—C6	−179.71 (11)	C11—N1—C7—O1	2.4 (2)
N2—C1—C2—C3	−179.26 (12)	C6—N1—C7—N2	−1.44 (13)
C6—C1—C2—C3	0.29 (18)	C11—N1—C7—N2	−177.93 (11)
C1—C2—C3—C4	−0.4 (2)	C7—N2—C8—C9	107.51 (15)
C2—C3—C4—C5	0.2 (2)	C1—N2—C8—C9	−73.46 (18)
C3—C4—C5—C6	0.2 (2)	C7—N1—C11—C12	88.90 (15)
C4—C5—C6—N1	179.75 (12)	C6—N1—C11—C12	−87.00 (15)
C4—C5—C6—C1	−0.37 (18)	N1—C11—C12—C17	99.61 (15)
C7—N1—C6—C5	−179.00 (12)	N1—C11—C12—C13	−81.60 (15)
C11—N1—C6—C5	−2.7 (2)	C17—C12—C13—C14	−0.6 (2)
C7—N1—C6—C1	1.11 (13)	C11—C12—C13—C14	−179.46 (13)
C11—N1—C6—C1	177.44 (11)	C12—C13—C14—C15	0.4 (2)
C2—C1—C6—C5	0.12 (17)	C13—C14—C15—C16	0.1 (3)
N2—C1—C6—C5	179.78 (10)	C14—C15—C16—C17	−0.5 (3)
C2—C1—C6—N1	−179.98 (11)	C13—C12—C17—C16	0.3 (2)
N2—C1—C6—N1	−0.32 (12)	C11—C12—C17—C16	179.09 (14)
C1—N2—C7—O1	−179.06 (13)	C15—C16—C17—C12	0.3 (3)
C8—N2—C7—O1	0.1 (2)		

Symmetry codes: (i) $x, y+1, z$; (ii) $-x, y+1/2, -z+1/2$; (iii) $x, -y+3/2, z-1/2$; (iv) $-x+1, -y+1, -z+1$; (v) $-x, -y+1, -z+1$; (vi) $x, y-1, z$; (vii) $-x+1, y+1/2, -z+1/2$.

Hydrogen-bond geometry (\AA , $^\circ$)

Cg2 is the centroid of the C1—C6 benzene ring.

$D—\text{H}\cdots A$	$D—\text{H}$	$\text{H}\cdots A$	$D\cdots A$	$D—\text{H}\cdots A$
C3—H3 \cdots O1 ⁱⁱⁱ	0.982 (18)	2.542 (18)	3.4997 (18)	165.1 (14)
C16—H16 \cdots O1 ^{vi}	0.994 (18)	2.568 (18)	3.468 (2)	150.6 (14)
C17—H17 \cdots Cg2 ^{viii}	1.00 (2)	2.831 (18)	3.6964 (17)	144.6 (15)

Symmetry codes: (iii) $x, -y+3/2, z-1/2$; (vi) $x, y-1, z$; (viii) $-x+1, y-1/2, -z+1/2$.